Development of a 3D Model for the Human Cannabinoid CB1 Receptor

Outi M. H. Salo,* Maija Lahtela-Kakkonen, Jukka Gynther, Tomi Järvinen, and Antti Poso

Department of Pharmaceutical Chemistry, University of Kuopio, P.O. Box 1627, FIN-70211 Kuopio, Finland

Received October 6, 2003

A novel comparison model of the human cannabinoid CB1 receptor has been constructed using the bovine rhodopsin X-ray structure as a template. The model was subjected to a 500-ps molecular dynamics simulation, and thereafter new conformers of the receptor model were produced in a simulated annealing procedure. Using an automated docking procedure, well-known cannabimimetic ligands were docked into six different model conformers, of which one was chosen for a detailed study of receptor−ligand interactions. The docking results confirm, for example, the importance of lysine K3.28(192) in the binding of these ligands. Also, other experimental data are fairly consistent with the present model, though there are some differences when compared to other recent CB1 comparison models. The present model will serve as a tool to investigate the receptor−ligand interactions and facilitate the design of novel cannabimimetic drugs.

Introduction

G-protein-coupled receptors (GPCRs) are important targets for drug discovery. To date, over 30% of the clinically marketed drugs are active at this receptor family.[1] GPCRs are integral membrane proteins that characteristically have seven α-helices spanning a membrane bridged by three intracellular and three extracellular loops. Either constitutively or by agonist binding, GPCRs activate different types of G proteins on the intracellular side of the lipid membrane and thus elicit a biochemical response through various signal transduction mechanisms. Cannabinoid receptors (subtypes CB1 and CB2) belong to Family A of GPCRs (Rhodopsin family, see http://www.gpcr.org/7tm), and they are an attractive target for current drug development. CB1 receptors are predominantly located in the central nervous system (CNS), whereas CB2 receptors have been discovered in peripheral tissues, such as the tonsils, spleen, and immunocytes.[2] Both receptor subtypes were cloned in the 1990s;[3,4] endogenous ligands for the cannabinoid receptors have also been characterized, including *N*-arachidonoylethanolamide[5] (AEA, **1**, Figure 1), 2-arachidonoylglycerol[6,7] (2-AG, **2**, Figure 1), noladin ether,[8] virodhamine,[9] and *N*-arachidonoyldopamine[10] (NADA). There are a few exogenous ligands for these receptors, of which the best-known is Δ^9-tetrahydrocannabinol[11] (THC), a product of *Cannabis sativa* L. In addition, several cannabinoid analogues and some structurally different cannabimimetic ligands have also been synthesized during the past two decades. Most of the therapeutic effects of cannabinoids and cannabimimetics, such as analgesia, lowering of intraocular pressure, antiemesis, alleviating of neuronal disorders, and stimulation of appetite, have been shown to be mediated through cannabinoid receptors, particularly through the CB1 receptor.[12]

In addition to the structure−activity relationships (SAR) of the receptor ligands, structural knowledge of the target receptor protein is important in facilitating drug design. Since cannabinoid receptors are transmembrane receptors, like all the GPCRs, elucidation of their three-dimensional (3D) structure has been highly demanding and not yet successful. The first 3D model of the CB1 receptor was based upon Fourier transform analyses of the α-helical periodicity in the sequences of the CB1 receptor and a set of homologous GPCRs.[13,14] The hydrophobic moments for each helix were calculated to arrive at their orientation in the bundle; additionally, the low-resolution projection structure of rhodopsin[15,16] and mutation data from other GPCRs were used to refine the model. Further refinement of this model included, for example, introducing new conformations of the sixth and seventh transmembrane helices (TM6 and TM7, respectively) into the CB1 helix bundle.[17] Another early CB1 model by Mahmoudian was based on the crystal structure of bacterial rhodopsin.[18] As

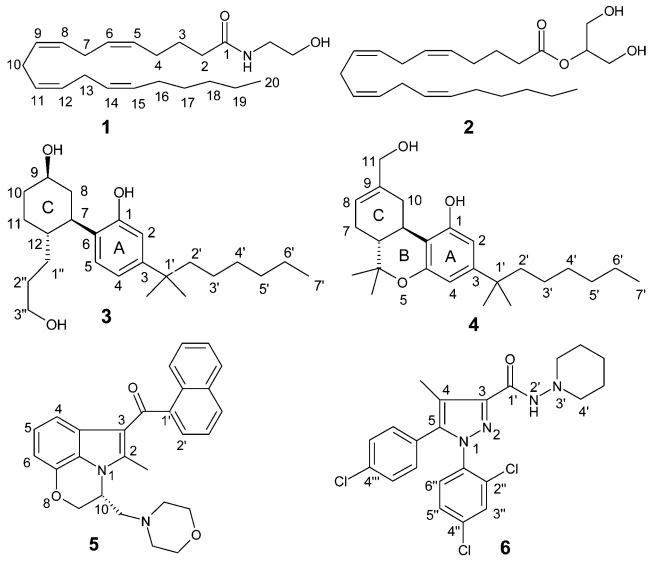

Figure 1. Molecular structures that were docked at the CB1 receptor model: (1) AEA, (2) 2-AG, (3) CP55940, (4) HU-210, (5) WIN55212-2, (6) SR141716A.

* To whom correspondence should be addressed. Tel.: +358-17-163714. Fax: +358-17-162456. E-mail: outi.salo@uku.fi.

10.1021/jm031052c CCC: $27.50
Published on Web 05/04/2004

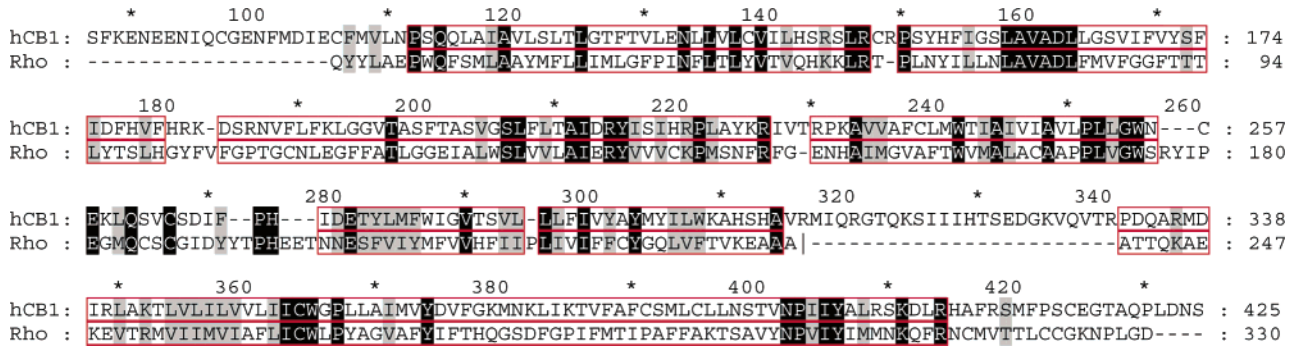

Figure 2. Modeling alignment of the human CB1 receptor (hCB1) and bovine rhodopsin (Rho) amino acid sequences. Highly conserved residues are marked with colored background; black, identical residues; gray, conservatively replaceable residues. Boxed regions denote the amino acid coordinates transferred from the rhodopsin X-ray structure onto the CB1 model. N- and C-terminals were left out of the model. "|" depicts the missing residues of the rhodopsin X-ray structure (i.e., AQQQES).

bacterial rhodopsin is not a GPCR,[16] and its helix-packing arrangement differs notably from that of GPCRs,[19] there was the need for a high-resolution crystal structure of a real GPCR.

Palczewski et al.[20] succeeded in determining the first, and thus far the only, crystal structure of a GPCR, that is, bovine rhodopsin. This crystal structure can be used as a structural template to model the transmembrane domain of other Family A GPCRs.[21] Ballesteros et al.[22] demonstrated that GPCRs maintain their general folding characteristics by means of structural mimicry, despite the possible low homology between these receptors. This structural mimicry also enables localized variations within the binding sites of the receptors that are responsible for the selectivity of a receptor toward a diverse group of ligands. However, Ballesteros and co-workers emphasize that substantial modifications of the initial template may be required to refine the particular conformation of the binding site for the exploration of specific ligand−receptor interactions. A study by Bissanz and co-workers[23] demonstrated that comparison (or homology) models of GPCRs can also be used as suitable targets for protein-based virtual screening of chemical databases.

The aim of the present study was to build a comparison model of the CB1 receptor in order to assist in the investigation of receptor−ligand interactions and in the design of novel selective CB1 ligands that could serve as potential lead molecules for cannabinoid-based drug discovery. Molecular dynamics simulations and automated ligand docking were used to refine and examine the receptor model. The resulting model is also compared to other recently published X-ray structure-based CB1 models.[24,25] The possible differences and/or similarities between these models are discussed.

Results and Discussion

Comparative Modeling. The core of the transmembrane (TM) helices of rhodopsin and CB1 sequences was well aligned (Figure 2), guided by highly conserved residues that are common to GPCRs.[26] Normally, gaps are avoided in the middle of the secondary structures of comparison models, but the multiple sequence alignment of hCB1 and other related sequences (see Supporting Information) gave an indication that the highly conserved proline residue P5.50(215) of rhodopsin could be omitted, as this is lacking in the CB1 sequence. The resulting gap in the CB1 model was repaired by joining the chain ends of the neighboring leucine residues L(286) [now given a locant of 5.50] and L5.51(287). Energy minimization of the resulting comparison model polished the backbone without extensively disturbing the helical structure at this particular point. Due to this procedure, the coordinates up to L5.50(286) in the TM5 were one residue behind, compared to the recent model built by Shim et al.[25] As this part of the helix is on the extracellular side, the binding site of our model is likely to differ from the model built by Shim et al. Particularly, in our model tyrosine Y5.39(275) of CB1, which has been shown to have a critical role in ligand recognition of cannabinoid receptors,[17] is in a position equivalent to F5.38(203) of rhodopsin, whereas Shim and co-workers aligned Y5.39(275) of CB1 with V5.39(204) of rhodopsin. McAllister and coauthors[17] compared their CB1 model with the rhodopsin X-ray structure and reported that Y5.39(275) of their CB1 model is in a position equivalent to F5.38(203) of rhodopsin, and in both receptors this tyrosine residue is engaged in an aromatic stacking interaction with W4.64(255). In addition to this particular stacking interaction, the other possible aromatic stacking interactions reported by McAllister et al.[17] for their wild-type CB1 model are also in line with the results of the present study.

Since the most challenging task has been to model the loops, which differ both in length and in amino acid order among the GPCRs, most reported 3D models of CB1 do not have all the six loops, if any.[13,17,18,24,25] The greater the difference in the length of the loop, the more difficult it is to model the loop in a reliable way. Nevertheless, we decided to model all the loops for a better theoretical view of the whole protein structure. The coordinates of the third extracellular (E3) loop were taken directly from the rhodopsin X-ray structure. Also, the first extracellular loop (E1) and the intracellular loops I1 and I2 were simple to model, as there was only one amino acid insertion or deletion needed with respect to the loops of rhodopsin. In all cases, as many amino acid coordinates as possible were taken from the rhodopsin structure, both before and after the gap region of the loop (see Figure 2).

The most difficult loops to reliably model were E2 and I3, as they differed most from the respective loops of rhodopsin. The random loop search for those regions gave us loop structures that may not, however, be identical to the real structure of CB1. Most GPCRs of the rhodopsin family have a disulfide bridge between

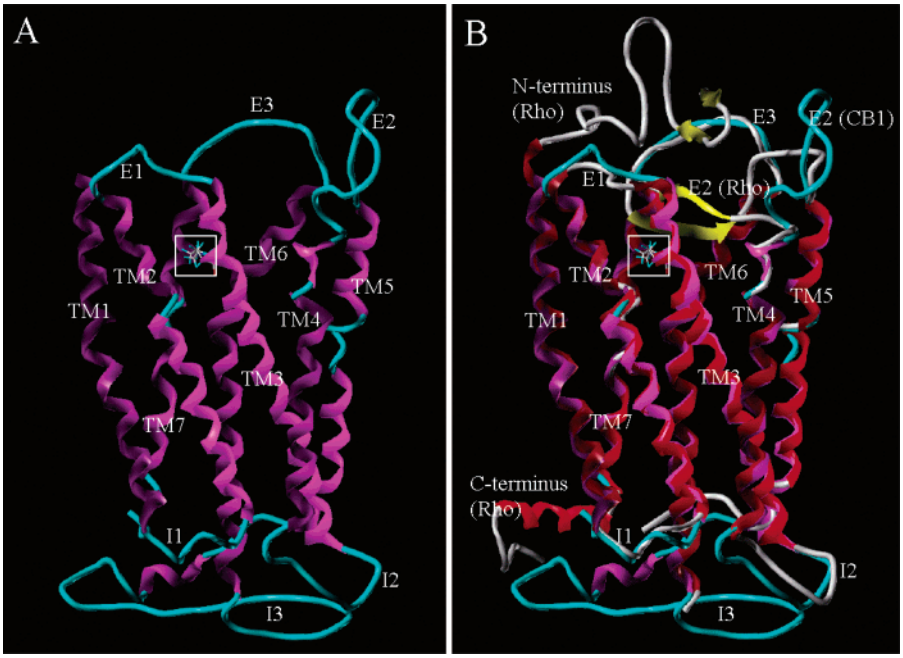

Figure 3. CB1 model compared with the rhodopsin crystal structure (Rho). The critical lysine K3.28(192) is boxed. Secondary structure coding: α-helix, purple (CB1)/red (Rho); *β*-sheet, yellow; other, cyan (CB1)/white (Rho). (A) CB1 model, (B) CB1 model superimposed with rhodopsin.

TM3 and E2.[27] In rhodopsin, this bridge draws the E2 loop down so that the loop covers the ligand binding site and, thus, is involved in ligand recognition. CB receptors lack this particular disulfide bridge. However, there is some evidence to suggest that a disulfide bridge is formed between the conserved cysteine residues of the E2 loop [in CB1 C(257) and C(264)] and that this loop region is important, for example, in the binding of CP55940 (**3**, Figure 1).[28−30] In the present model, this possible disulfide bridge was not taken into account, in order to focus solely on the cannabinoid binding site within the helix bundle.

Figure 3 presents the CB1 model (model 1, see Experimental Section) compared with the rhodopsin crystal structure. The secondary structures were assigned as implemented by SYBYL. One can clearly see how the E2 loop of rhodopsin bends over the ligand binding site (Figure 3B). The loop is almost at the same level as the critical K3.28(192) residue. As expected, deviations from the ideal α-helical structure are located in the respective TM regions of both the receptors. However, in the CB1 model the TM5 region of deviation is a few residues longer than in rhodopsin due to the omission of the P5.50 coordinates (see text above). On the other hand, the regions of deviation from the ideal α-helix in TM7 and at the end of TM4 are longer in rhodopsin compared with those regions in the CB1 model.

Molecular Dynamics. The MD simulations with TIP4P water in the OPLS force field were extensively time-consuming, but they resulted in structures of slightly better stereochemical quality when compared with the SPC simulations in the Gromacs force field. The Ramachandran plot[31] of the SPC model for CB1 revealed four residues in the disallowed region, one of them [V3.32(196)] being in the TM3 near the putative binding site. In the Ramachandran plot of the TIP4P model, there were only two residues in the disallowed

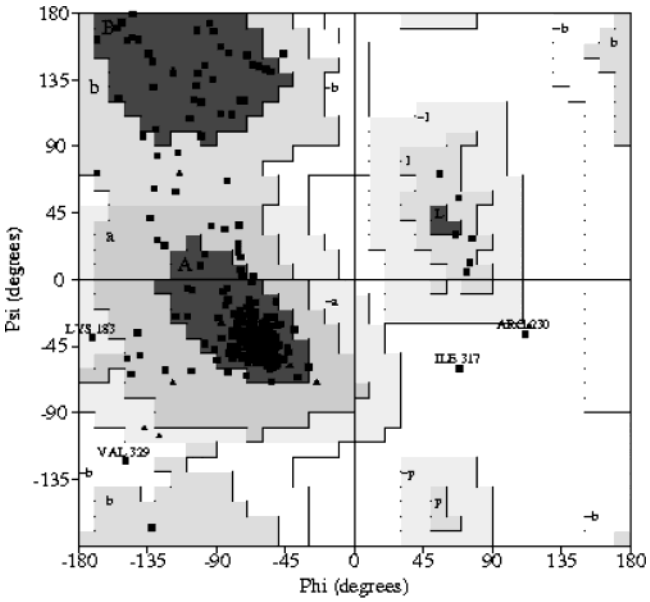

Figure 4. Ramachandran plot for the CB1 final structure from TIP4P molecular dynamics simulation. The following residues were in the disallowed region: I(317) and R4.39(230).

region, both being far away from the binding site: I(317) in the I3 loop and R4.39(230) at the cytoplasmic end of TM4 (Figure 4). Although in the TIP4P model the stereochemistry of residue V2.55(168) had changed from L to D, inverting the chirality back to the L-amino acid did not affect the structure of the binding site, as this residue points out toward the lipid membrane. Similar results were obtained for the rhodopsin X-ray structure; that is, there were two residues in the disallowed region of the SPC model but none in the TIP4P model. Otherwise, the stereochemical quality of the CB1 model was comparable with that of the rhodopsin structure. (See Supporting Information for the PROCHECK summaries.) Eventually, the decision to use structures from

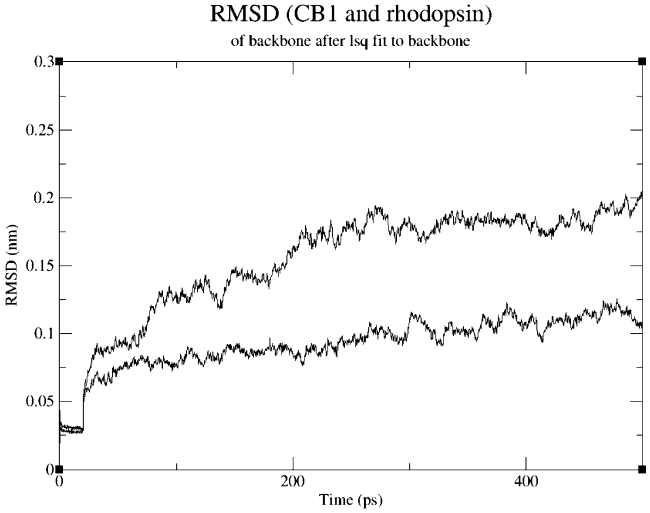

Figure 5. Rmsd fluctuations of the protein backbones during simulation: CB1 model (above) vs crystal structure of bovine rhodopsin (below).

the TIP4P MD simulation was confirmed by the fact that, during the SPC simulation, the critical lysine K3.28(192) tended to rise up and thus point outward from the binding site.

The MD simulation of the CB1 model was stable, as there was no drift in the energy or temperature. The root-mean-squared deviation (rmsd) of the protein backbone was plotted over the simulation time for the CB1 model and the crystal structure of bovine rhodopsin after a least-squares fit to the initial structure (Figure 5). Even though the deviation increases to about 2 Å for the CB1 model, compared to a deviation of 1 Å for the rhodopsin structure, both receptor structures remained stable. Most of the deviation was due to moving loops, as the backbone of the CB1 loop region fluctuated up to 4 Å compared with the restrained helix area, in which the backbone rmsd remained at about 0.5 Å (see Supporting Information, Figure 1). In the CB1 model, the loops (especially E2 and I3) were probably not as they exist in the real protein; thus, they are not so well packed, which causes a greater rms deviation compared to the crystal structure. The overall deviation would possibly increase if the position restraints of the helix backbone atoms were loosened. However, this should be done in a real lipid membrane environment and not in a system of pure water. Even though it is argued that, by the current computational methods, it is not possible to simulate the complete event of the receptor activation,[32] a free simulation of the receptor model in a lipid membrane might give some insight, as the helices will be allowed to move freely. For example, TM6 is proposed to straighten upon activation.[33,34]

It is a well-known fact that bovine rhodopsin was crystallized in its inactive state.[20] Therefore, it may be assumed that the initial CB1 model also represents the inactive receptor conformation. Singh and co-workers[35] studied the reason for the high constitutive activity of the CB1 receptor compared to the complete lack of constitutive activity in rhodopsin. When rhodopsin is activated, the aromatic residue W6.48 is proposed to undergo a rotameric shift of the $\chi 1$ torsion angle from gauche+ to trans. Singh et al. suggest that in CB1, the trans $\chi 1$ rotamer of W6.48(356) is favored due to the greater conformational mobility of this residue compared with that of W6.48 of rhodopsin. They also propose that the rotameric state of F3.36(200) controls the rotamer switch of W6.48(356), so that the trans $\chi 1$ rotamer of F3.36 helps to constrain W6.48 in a gauche+ $\chi 1$, but the gauche+ $\chi 1$ configuration of F3.36 allows W6.48 to shift to trans $\chi 1$. Interestingly, this rotamer switch was also confirmed in the present study. Before the MD simulation, W6.48(356) was in the gauche+ $\chi 1$ configuration, as in the rhodopsin template. In the process of comparative modeling, the HOMOLOGY module of InsightII chose the gauche+ $\chi 1$ rotamer for F3.36(200), which is a glycine residue in rhodopsin. During the MD simulation of the CB1 model, the rotamer of W6.48(356) shifted from gauche+ $\chi 1$ to trans $\chi 1$ (Figure 6), in contrast to the respective simulation for rhodopsin.

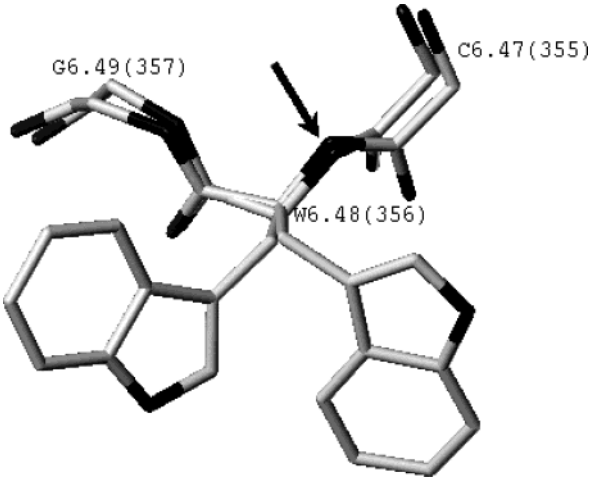

Figure 6. Rotamer shift of W6.48(356) from gauche+ $\chi 1$ to trans. The backbone nitrogen is shown with an arrow. When viewed from this side of the backbone, the side-chain γ carbon for the trans rotamer is at a position opposite to the backbone nitrogen, whereas for the gauche+ rotamer the γ carbon is on the same side as the backbone nitrogen.

Docking of Ligands. All of the best-ranked (CScore value of 3−5) docking conformations of the ligands were visually checked in every receptor conformer. Model 1 was chosen for the detailed discussion of the ligand−receptor interactions. In that receptor conformation, the binding site was the most open, and it was not as fragmented as in the conformers produced by the simulated annealing procedure. Due to the openness of the binding cavity, the ligands found more different docking positions in model 1 than in models 3−6. In some cases, this enabled a certain ligand to interact with a certain amino acid that was inaccessible in models 3−6. Moreover, WIN55212-2 seemed to find better docking conformations at model 1 than at model 2. The structure of model 1 also agreed well with the average structure calculated from the MD simulation. All six ligands were found to be docked approximately into the same area of the binding cavity (Figure 7). It has been proposed that there is a partial overlap between the binding sites of structurally different cannabinoids.[29]

Mutation data have shown that lysine K3.28(192) is an important residue for the binding of AEA.[36] Consistently, we chose a docking conformation for both AEA and 2-AG that involved a hydrogen-bonding interaction (see Table 1 for H-bond distances and angles) between

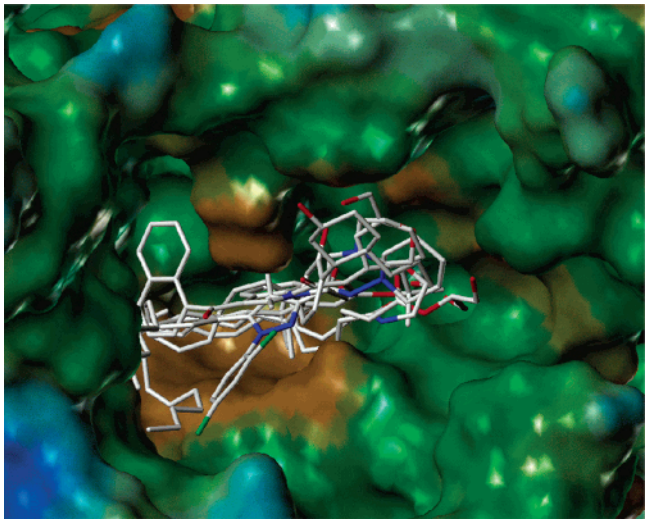

Figure 7. Docked ligands at the binding site of the CB1 model (view from the extracellular side). MOLCAD lipophilic potential surface was calculated for the model with the Connolly method.[77] Brown color denotes the most lipophilic areas and blue denotes the most polar areas. Ligand atoms have been colored in the following way: gray, carbon; red, oxygen; blue, nitrogen; green, chlorine. Hydrogens have been left out for clarity.

the carbonyl oxygen of the ligand and the lysine nitrogen of the receptor (Figure 8A). It is possible that the headgroup hydroxyls of the ligands form simultaneous H-bonds with K3.28(192) or intramolecular H-bonds with the carbonyl oxygen. In our model, S7.39-(383) was located opposite to the critical lysine and may also be involved in forming H-bonds with the polar headgroups of the ligands (Table 1). Both endocannabinoids adopt a U-shaped molecular conformation, with their aliphatic tails turning to the lipophilic region of the binding site. In this conformation, the ligand acyl chain is located in the vicinity of residues such as F3.36-(200), W5.43(279), and L5.40(276). However, no specific C—H···π interactions were recognized between the hydrogens of the aromatic rings and the double bonds of AEA in this binding model (see Supporting Information). This finding is consistent with the site-directed mutation data from McAllister and co-workers, which shows that AEA binding does not change when amino acids F3.36(200) and W5.43(279) are mutated into alanine.[37,38] Nevertheless, it was reported that the potency and/or efficacy of AEA is reduced after the above-mentioned mutations.[37] Therefore, it is possible that these residues are not important for the recognition of AEA but are important for the activation of the receptor. Barnett-Norris and co-workers[24] reported that F2.57(170) and F3.35(189) interact with the double bonds of the endocannabinoid acyl chain. Their finding is supported by the experimental fact that replacing F3.25(189) with alanine decreases the CB1 binding affinity of AEA by 7-fold.[24] In a recent study by McAllister et al.,[38] F3.25(189)A mutation resulted in a 6-fold loss in CB1 affinity for AEA. Their modeling studies suggest that F3.25(189) has a C—H···π interaction with the C5═C6 bond of AEA, and that F2.57(170) interacts with the amide oxygen of AEA, whereas in the present model the chosen conformer of AEA does not have any interactions with F3.25(189).

K3.28(192) is also important for the binding of HU-210 and CP55940. Being a very flexible residue, it can easily adopt a conformation that interacts with the phenolic hydroxyl, northern aliphatic hydroxyl (C9/C11 hydroxyl), southern aliphatic hydroxyl (SAH, C12 hydroxypropyl of CP55940), or even the pyranyl oxygen of classical cannabinoids.[39] Docking HU-210 and CP55940 into our model gave many putative binding conformations for these two ligands. In some conformations, the C3 alkyl chain was pointing out of the receptor cavity, while in some conformations it was bending into the hydrophobic region of the binding site. Representative conformers, in which the side chain was positioned into the hydrophobic part of the binding pocket, are presented in Figure 8B. In this conformation, the SAH group of CP55940 and the pyranyl oxygen of HU-210 can come within hydrogen-bonding distance of K3.28-(192) (see Table 1). Also, S7.39(383) may hydrogen bond with the pyranyl oxygen. With a light rotation of the lysine residue, it can easily reach the phenolic hydroxyl of HU-210 as well. The northern aliphatic hydroxyl groups of these cannabinoids and the phenolic hydroxyl group of CP55940 do not have any specific interaction sites in this conformation. Shim and co-workers[25] studied the binding mode of nonclassical cannabinoid agonists such as CP55940 in their CB1 model. They concluded that a binding conformation in which the C3 alkyl tail is pointing inside the receptor was marginally better than a conformation with the alkyl tail pointing out toward the extracellular side of the receptor. In this conformation, the nonclassical cannabinoid agonists would hydrogen bond with K3.28(192) and E(258), as well as with Q(261), by involving their phenolic hydroxyl and the SAH groups, respectively. In contrast to our model, this model gives insight into the ligand interactions with residues of the E2 loop, as this loop has been modeled with the disulfide bridge and is bending over the binding site. The following residues are reported to form a hydrophobic pocket for the C3 alkyl tail: V3.32-(196), T3.33(197), F3.36(200), L(260), F5.42(278), W6.48-(356), L6.51(359), M6.55(363), and C7.42(386). In our model, for the conformation discussed, the respective amino acid residues (within 2.5 Å of the bound ligand) are V3.32(196), T3.33(197), F3.36(200), Y5.39(275), W5.43(279), L6.51(359), and M6.55(363). Mutation studies have demonstrated that interactions with F3.25-(189), F3.36(200), W5.43(279), and W6.48(356) are not critical for the binding of CP55940.[37,38] Residue F3.25-(189) is located in the vicinity of the cyclohexyl ring of CP55940, but there is no strong interaction between the ligand and this residue in the present model. Interactions with F3.36(200) and W5.43(279) are mainly through van der Waals interactions with the dimethylheptyl side chain of CP55940. The only aromatic stacking interaction that CP55940 has in the present binding model is with F7.35(379) (d = 5.8 Å; α = 30°). Hart et al. examined the binding mode of (+)-7-OH-CBD-DMH, a dimethylheptyl analogue of cannabidiol, in their CB1 model.[40] They found that the TM2-3 region forms a binding site for this ligand. Specifically, K3.28(192) formed a hydrogen bond with one phenolic hydroxyl group and S2.60(173) formed a hydrogen bond with the second phenolic hydroxyl, while the 7-hydroxyl formed a hydrogen bond with Y2.59(172).

Table 1. Hydrogen-Bonding Interactions for the Chosen Conformations of the Docked Cannabinoid Ligands at Model 1

ligand	donor	acceptor	d_{DA}[a] (Å)	α_1[a] (deg)	α_2[a] (deg)
AEA	K3.28	carbonyl oxygen of AEA	2.7	111	115
		hydroxyl oxygen of AEA	3.2	165	109
	S7.39	carbonyl oxygen of AEA	3.0	118	89[b]
2-AG	K3.28	carbonyl oxygen of 2-AG	2.4	152	160
	S7.39	ester oxygen of 2-AG	3.2	141	87/104
CP55940	K3.28	SAH[c] oxygen of CP55940	2.3	126	119
HU-210		pyranyl oxygen of HU-210	2.5	121	97/102
WIN55212-2[d]		O8 of WIN55212−2	2.3	140	111/128
SR141716A[e]		carbonyl oxygen of SR141716A	2.4	149	101

[a] See Experimental Section for definition. [b] Slightly smaller than the limit value (90°). [c] SAH = southern aliphatic hydroxyl (i.e., C12 hydroxypropyl of CP55940). [d] Experimental data have shown that lysine K3.28(192) is not necessary for the binding of WIN55212-2.[36,43] [e] SR141716A docked at model 7.

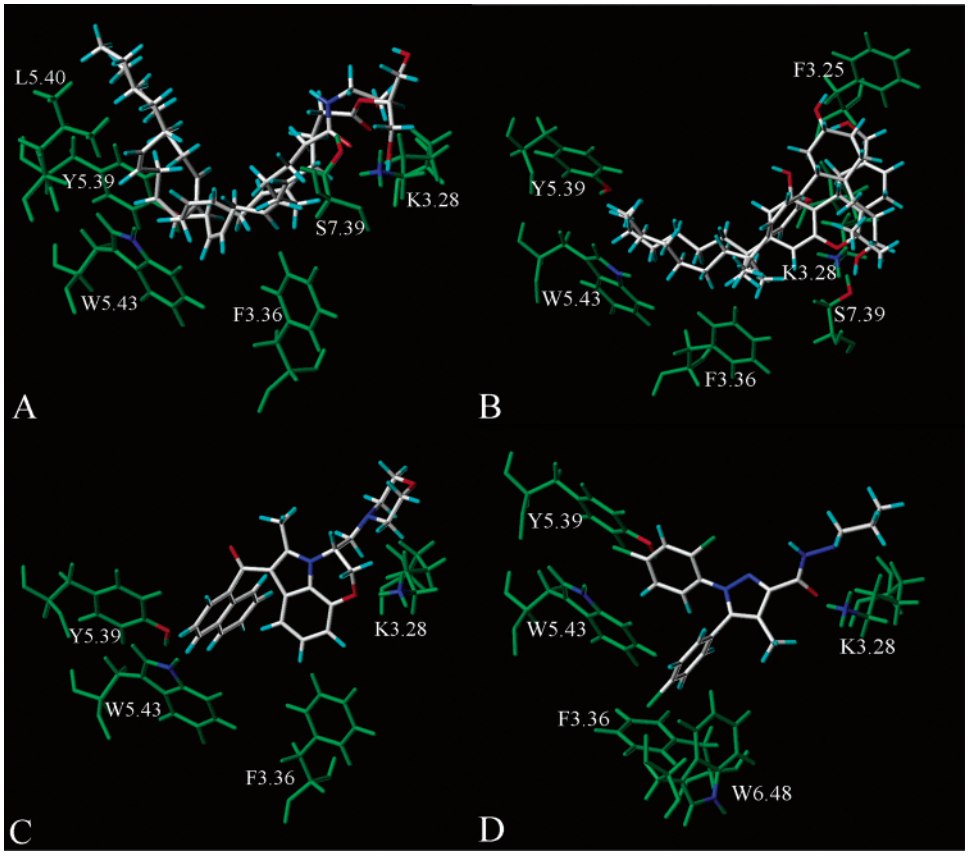

Figure 8. Representative docking conformations of the cannabinoid ligands (see text). Receptor residues are colored green, except for the heteroatoms of the side chains. Ligand color code: gray, carbon; red, oxygen; blue, nitrogen; green, chlorine. (A) AEA and 2-AG, (B) HU-210 and CP55940, (C) WIN55212-2, (D) SR141716A.

CB1/CB2 chimera studies have shown that the TM4-E2-TM5 region of cannabinoid receptors is important for the binding of WIN55212-2.[29] Combined mutation and modeling studies by Song and co-workers support the importance of aromatic stacking for WIN55212-2 interaction with cannabinoid receptors.[14] In their model, the aromatic residues W4.64(255), Y5.39(275), F5.42-(278), F3.25(189), F3.36(200), and F5.43(279) were identified as forming the binding site for WIN55212-2, with the latter three residues being in direct interaction with WIN55212-2. Cannabimimetic indoles that are closely related to aminoalkylindoles such as WIN55212-2 were docked into the bovine rhodopsin-based CB1 model constructed by Barnett-Norris et al.[24,41] In particular, tryptophans W5.43(279) and W6.48(356) were involved in aromatic stacking with the naphthyl group and the indole nucleus of the docked ligands. Additionally, the N−H of W5.43(279) was found to form a hydrogen bond with the carbonyl oxygen for some of the cannabimimetic indoles. A hydrophobic binding pocket for the N1 alkyl substituent was comprised of V3.32(196), T3.33-(197), F3.36(200), L6.51(359), and I6.54(362). In the model used by Shim and co-workers, WIN55212-2 was reported to interact with a region in TM4, E2, and TM5.[42] Recently, McAllister et al.[37,38] reported a combined mutagenesis and modeling study of specific CB1 ligand−receptor interactions. Replacing the aromatic residues F3.36(200), W5.43(279), and W6.48(356) with alanine resulted in a significant loss of affinity for both WIN55212-2 and SR141716A, which underscores the importance of these native residues for the binding of WIN55212-2 and SR141716A. In contrast to the earlier study by Song and co-workers,[14] F3.25(189) was not found to interact with WIN55212-2, as replacing it with alanine did not have a significant effect on WIN55212-2 binding. Modeling studies by McAllister et al.[37,38] sug-

Table 2. Aromatic Stacking Interactions of WIN55212-2 (WIN) and SR141716A (SR)

		F3.36(200)		Y5.39(275)		W5.43(279)		W6.48(356)	
ligand	interacting group	d^a (Å)	α^a (deg)	d (Å)	α (deg)	d (Å)	α (deg)	d (Å)	α (deg)
WIN[b]	indole	5.5	9	–[c]	–	–	–	–	–
	naphthyl	–	–	5.4	48	5.2	73	–	–
SR[d]	monochloro	5.1	74	–	–	4.6	77	4.3	42
	dichloro	–	–	6.2	24	4.3	29	–	–

[a] See Experimental Section for definition. [b] WIN55212-2 docked at model 1. [c] –, Distance exceeds the 7 Å criteria for aromatic stacking interactions. Angle not determined. [d] SR141716A docked at model 7.

gest that the naphthyl ring of WIN55212-2 has a direct aromatic stacking interaction with F3.36(200), W5.43-(279), and W6.48(356), and that the indole ring of WIN55212-2 also stacks with F3.36(200). In the present study, the distances and geometry of the aromatic stacking interactions are shown in Table 2. The indole core of WIN55212-2 has an offset parallel stack with F3.36(200), and the naphthyl group stacks directly with W5.43(279) and Y5.39(275) (Figure 8C), whereas the intervening amino acids prevent stacking interactions with W6.48(356) in the present binding model. A hydrogen bond between O8 of WIN55212-2 and the side-chain nitrogen of K3.28(192) is also possible for the chosen binding conformation (Table 1). However, this is inconsistent with CB1 mutation studies that show K3.28(192) is not necessary for the effective binding of WIN55212-2.[36,43] Docking WIN55212-2 to a K192A mutant led us to conclude that lysine is not necessary for the binding of this ligand, as the strengthened aromatic interactions and the overall increase in hydrophobicity of the binding cavity can compensate for the loss of the H-bond in this binding model (see Supporting Information).

All the other ligands docked into our model were cannabinoid receptor agonists, but SR141716A is considered to be a selective CB1 antagonist that has been reported to act as an inverse agonist at the CB1 receptor.[44] Antagonists are thought to bind to the inactive conformation of the receptor. Our model was originally based on the inactive form of bovine rhodopsin. The transmembrane helix bundle was not modified in a way comparable to the active model constructed by Barnett-Norris and co-workers.[24] In that study, the TM3 and TM6 helices were rotated, and a less-kinked TM6 conformer based on the experimental results from rhodopsin and the β2-adrenergic receptor was used. Contrary to expectations that SR141716A would easily find good docking conformations, we found that most of the best-ranked conformations were not in line with the existing experimental evidence. Specifically, studies on chimeric CB1/CB2 receptors have demonstrated that the region delineated by the fourth and fifth transmembrane helices is crucial for high-affinity binding of SR141716A, though the E2 loop was not found to affect its binding.[30] Also, McAllister and co-workers reported that mutating F3.36(200), W5.43(279), and W6.48(356) to an alanine residue had a significant effect on the binding of SR141716A.[38] Results from a recent 3D-QSAR modeling of SR141716A suggest that the N1 or C5 aryl ring moiety of this ligand is important for its hydrophobic docking into the receptor pocket.[45] In the present study, only a conformer with a CScore value of 2 docked at model 1 in a way that the aromatic rings of SR141716A were interacting with the same aromatic region as WIN55212-2. Supposedly, conformational changes in the binding site during the MD simulation (especially the gauche+ χ1 to trans χ1 shift of the W6.48(356) rotamer) have an effect on SR141716A binding. Therefore, an additional receptor conformer (model 7, see Supporting Information for details) was made, where the rotameric states of W6.48(356) and F3.36(200) were set to the suggested inactive states,[35] gauche+ and trans, respectively. SR141617A was docked into this model, and the interactions of the best-scored docking conformation (CScore 5) were examined in detail. In model 7, SR141716A has two direct stacking interactions with W5.43(279) and one direct stacking interaction with F3.36(200), W6.48(356), and Y5.39(275) (Table 2, Figure 8D). Consistent with the results of Hurst and co-workers, in this docking conformation of SR141716A, lysine K3.28(192) forms a hydrogen bond with the carbonyl group of SR141716A (Table 1).[46] This hydrogen bonding of the SR141716A C3 substituent is suggested to be responsible for the higher affinity of SR141716A to the inactive receptor state, leading to its inverse agonism. Hurst et al. also reported that, in their modeling studies, SR141716A was involved in aromatic stacking interactions with F3.36(200), Y5.39(275), and W5.43(279). In their model, a salt bridge between K3.28-(192) and D6.58(366) made K3.28(192) available for hydrogen-bonding interaction.

To the authors' knowledge, the present model is the first bovine rhodopsin-based CB1 model to be reported together with automated docking results for ligands at this receptor site. The bias toward a particular result is smaller in automated docking than in manual or semimanual docking. For example, in the present study the radius of the cavity around the lysine 192 nitrogen was determined to be 18 Å; therefore, this critical lysine was not necessarily part of every suggested docking position. However, it was confirmed that automatically docked ligands were able to find this residue and even to form a hydrogen bond with its side-chain nitrogen. The conformation of the binding-site residues did affect the docking results significantly, but, overall, these results are fairly consistent with the experimental data.

Conclusions

A comparison model of the human cannabinoid CB1 receptor was constructed to obtain information on the receptor–ligand interactions at the putative ligand-binding site and, thus, to facilitate the design of novel lead compounds for current cannabimimetic drug discovery. After the model receptor structure was subjected to a 500-ps MD simulation in an aqueous system with constrained helix backbone atoms, different conformations of the binding site were produced in a simulated annealing procedure. A total of six distinct conformers

(models 1−6) were chosen for the ligand docking studies. AEA, 2-AG, CP55940, HU-210, WIN55212-2, and SR141716A were docked automatically into these six different receptor conformers. Model 1 was chosen for closer examination of the docking results.

The results confirm that lysine K3.28(192) plays a significant role in the binding mode of most studied ligands, and that aromatic stacking is an important type of interaction for WIN55212-2 and SR141716A. The model is fairly consistent with previous mutational studies and shares common features with recent CB1 models constructed by other groups. A careful examination of the receptor−ligand interactions revealed that there are some differences between current models, due to the different ways of constructing the studied receptor. In addition, other groups have used manual or semimanual docking instead of the automated docking as in the present study. It is possible that there are different conformations of the CB1 receptor that bind different types of cannabimimetic ligands under physiological conditions. However, in the absence of crystallized receptor−ligand complexes, such models, though imperfect pictures of the reality, can still give valuable information on the receptor−ligand interactions.

Experimental Section

Methods. Sequences were retrieved from the SWISS-PROT protein sequence database,[47] and the crystal structure of bovine rhodopsin was taken from the Protein Data Bank (PDB).[48] The multiple sequence alignment was performed with CLUSTAL W[49,50] using the Blosum series as a matrix. Structure construction, optimization, and visualization were carried out using the molecular modeling packages SYBYL[51] and InsightII.[52] Specifically, the HOMOLOGY module of InsightII was used for the process of comparative modeling. Energy minimization of the modeled structure was done by steepest descent and conjugate gradient methods (as implemented by SYBYL), using Kollman United[53] or Kollman All-Atom force fields[54] with Kollman charges.[55] Molecular dynamics (MD) simulations were performed by using the GROMACS package.[56,57] Ligand docking was performed with GOLD,[58] and the CScore[59] module of SYBYL was implemented to calculate and rank the docking scores for the resulting docking conformations. The stereochemical quality of the resulting protein structures was tested with the PROCHECK[60] computer program.

Amino Acid Numbering. To refer to specific amino acids in the CB1 receptor sequence, the amino acid numbering system suggested by Ballesteros and Weinstein[61] is used. The most highly conserved amino acid residue in each helix of a GPCR is assigned a locant value of 0.50. This value serves as a reference amino acid position, so the other residues in the helix are given a locant value relative to it. The preceding number in the amino acid identifier indicates the number of the helix, and the following number, in parentheses, gives the sequence number. For example, G6.49(357) is a glycine that is at position 357 in the CB1 receptor sequence, and it precedes the most highly conserved residue, P6.50(358), in the sixth transmembrane helix (TM6).

Comparative Modeling. The crystal structure of bovine rhodopsin (PDB code 1hzx, solved at a resolution of 2.8 Å)[62] was used as the template for the comparative modeling process. Initially, a BLAST[63,64] search in the SWISS-PROT database was done in order to find sequences that were homologous with the human CB1 receptor sequence (hCB1). Thereafter, the sequence of the hCB1 was aligned with the sequence of bovine rhodopsin and 12 other homologous GPCRs.[65] The identities of the aligned sequences varied between 23% and 97% with the human CB1 sequence, rhodopsin being the least homologous. The resulting multiple sequence alignment (see Supporting Information) was compared with the highly conserved amino acids of GPCRs, as reported by Baldwin.[26] Additionally, different algorithms were used to predict the residues compiling the seven transmembrane helices (see Supporting Information). These data were used to determine the final modeling alignment of hCB1 and rhodopsin sequences (Figure 2).

The transmembrane helix coordinates were extracted from the rhodopsin X-ray structure, but the loops were generated by the loop search procedure of InsightII, which utilizes the structures deposited in PDB. However, the coordinates of the third extracellular loop (E3) were taken directly from rhodopsin, as this loop was of similar length in the CB1 receptor. The amino acid coordinates transferred from rhodopsin onto the CB1 model are shown in Figure 2. Finally, the model was subjected to a limited energy minimization (see Methods) to remove any unfavorable steric interactions.

Molecular Dynamics. For the purpose of examining the stability of the model, a molecular dynamics (MD) simulation was performed on the receptor structure. Instead of using a real lipid bilayer for the simulation, the modeled structure was placed in a cubic water box at 300 K for 500 ps (after a 20-ps equilibration of the system with all the heavy atoms of the protein constrained). Particle mesh Ewald (PME)[66] electrostatics and periodic boundary conditions were used in the simulation, as well as pressure and temperature coupling[67] to an external bath (see Supporting Information for the detailed MD parameters). We utilized the TIP4P[68] water model in the OPLS force field[69,70] and also performed a comparable MD analysis with the SPC[68] water in the Gromacs[57,71] force field. To mimic the lipid membrane, the backbone atoms of the helices were constrained with a force constant of 1000 kJ/(mol nm^2) so that only the loops and the helix side chains were able to move freely during the simulation. For comparison, similar MD simulations were performed on the rhodopsin X-ray structure. In the middle of the CB1 molecular dynamics run (with TIP4P water), two structures were randomly extracted from the simulation trajectory at 381 and 459.8 ps. After the simulations were completed, the final and intermediate structures were energy-minimized. Finally, average structures covering the 300−500 ps time span of the trajectories were calculated.

Simulated Annealing Procedure. In an attempt to explore the structural space of the putative cannabinoid binding site, 100 different conformations of the CB1 receptor model were produced in a simulated annealing procedure by heating the initial structure (extracted from MD simulation at 459.8 ps) at 1000 K. Only the side chains of the residues within a sphere of 20 Å surrounding the critical lysine residue K3.28(192)[36] were allowed to move during the process. In addition, a distance constraint of 14.5 Å with a constant of 50 (as implemented by SYBYL) was applied between the lysine 192 nitrogen and the backbone nitrogen of proline P6.50(358). This was to avoid unfavorable conformations of the critical lysine, where it turns up, pointing out of the binding cavity, and can form hydrogen bonds with polar residues of the E1 extracellular loop or TM2/TM3 helix-end residues (a phenomenon recognized in our vacuum simulations; data not shown). Subsequently, the resulting conformers of the receptor were energy-minimized, and both van der Waals and electrostatic fields were calculated for the putative binding site of the receptor with an in-house software. On the basis of these fields, the conformers were divided into four distinct groups with the help of the Visual Data[72] program, which uses the SOM[73] (self-organizing map) principle. From each group, one representative conformer was randomly picked for the docking studies.

Docking of Ligands. Six different receptor conformations were used for the docking studies: two receptor conformations obtained from the MD simulation trajectory (i.e., the snapshot taken at 381 ps [model 1] and the final frame of 500 ps [model 2]), and the remaining four (models 3−6) chosen from the simulated annealing procedure as described above. Well-known cannabinoid receptor ligands (**1**, **2**, CP55940 [**3**], HU-210 [**4**], WIN55212-2 [**5**], and SR141716A [**6**]; Figure 1) were selected for docking at these different conformers of the

receptor model. The ligands were automatically docked into the 18-Å cavity surrounding the side-chain nitrogen of lysine K3.28(192). The GOLD program was allowed to produce up to 25 different docking conformations for each ligand. All docking conformations in the different receptor conformers were then relaxed and ranked with CScore, and the conformations with the best scores were checked visually.

Ligand−Receptor Interactions. Hydrogen bonds were characterized with the following values: d_{DA}, the distance between the donor atom (D) and the acceptor atom (A); α_1, the angle determined by the donor atom, the hydrogen atom (H) attached to the donor, and the acceptor atom (D−H−A); and α_2, the angle determined by the hydrogen atom attached to the donor, the acceptor atom, and the heavy atom attached (X) to the acceptor (H−A−X). According to the hydrogen bond criteria,[74] d_{DA} should be less than 3.9 Å and both angles greater than 90°.

Receptor residues and ligands have been reported to participate in aromatic stacking interactions if the centroid-to-centroid distance (d) between the aromatic rings was within the range of 4.5−7.0 Å and the angle (α) between normal vectors of interacting rings within 30−90° in a tilted arrangement and smaller than 30° in an offset parallel arrangement.[75,76]

Acknowledgment. This work was supported by ISB (The National Graduate School in Informational and Structural Biology) and National Technology Agency of Finland. CSC Scientific Computing, Ltd., is gratefully acknowledged for computational resources. We also thank Toni Rönkkö (M.Sc.) for technical assistance.

Supporting Information Available: Among others, multiple sequence alignment, prediction of the TM helix residues of CB1, MD parameters, PROCHECK summaries, and schematic diagrams of the ligand−receptor interactions. This material is available free of charge via the Internet at http://pubs.acs.org. Coordinates for the receptor model in the present study are available from the corresponding author upon request.

References

(1) Wise, A.; Gearing, K.; Rees, S. Target validation of G-protein coupled receptors. *Drug Discovery Today* **2002**, *7*, 235−246.
(2) Pertwee, R. G. Pharmacology of cannabinoid CB1 and CB2 receptors. *Pharmacol. Ther.* **1997**, *74*, 129−180.
(3) Matsuda, L. A.; Lolait, S. J.; Brownstein, M. J.; Young, A. C.; Bonner, T. I. Structure of a cannabinoid receptor and functional expression of the cloned cDNA. *Nature* **1990**, *346*, 561−564.
(4) Munro, S.; Thomas, K. L.; Abu-Shaar, M. Molecular characterization of a peripheral receptor for cannabinoids. *Nature* **1993**, *365*, 61−65.
(5) Devane, W. A.; Breuer, A.; Sheskin, T.; Jarbe, T. U.; Eisen, M. S.; Mechoulam, R. A novel probe for the cannabinoid receptor. *J. Med. Chem.* **1992**, *35*, 2065−2069.
(6) Sugiura, T.; Kondo, S.; Sukagawa, A.; Nakane, S.; Shinoda, A.; Itoh, K.; Yamashita, A.; Waku, K. 2-Arachidonoylglycerol: a possible endogenous cannabinoid receptor ligand in brain. *Biochem. Biophys. Res. Commun.* **1995**, *215*, 89−97.
(7) Mechoulam, R.; Ben-Shabat, S.; Hanus, L.; Ligumsky, M.; Kaminski, N. E.; Schatz, A. R.; Gopher, A.; Almog, S.; Martin, B. R.; Compton, D. R.; Pertwee, R. G.; Griffin, G.; Bayewitch, M.; Barg, J.; Vogel, Z. Identification of an endogenous 2-monoglyceride, present in canine gut, that binds to cannabinoid receptors. *Biochem. Pharmacol.* **1995**, *50*, 83−90.
(8) Hanus, L.; Abu-Lafi, S.; Fride, E.; Breuer, A.; Vogel, Z.; Shalev, D. E.; Kustanovich, I.; Mechoulam, R. 2-arachidonyl glyceryl ether, an endogenous agonist of the cannabinoid CB1 receptor. *Proc. Natl. Acad. Sci. U.S.A.* **2001**, *98*, 3662−3665.
(9) Porter, A. C.; Sauer, J. M.; Knierman, M. D.; Becker, G. W.; Berna, M. J.; Bao, J.; Nomikos, G. G.; Carter, P.; Bymaster, F. P.; Leese, A. B.; Felder, C. C. Characterization of a novel endocannabinoid, virodhamine, with antagonist activity at the CB1 receptor. *J. Pharmacol. Exp. Ther.* **2002**, *301*, 1020−1024.
(10) Huang, S. M.; Bisogno, T.; Trevisani, M.; Al-Hayani, A.; De Petrocellis, L.; Fezza, F.; Tognetto, M.; Petros, T. J.; Krey, J. F.; Chu, C. J.; Miller, J. D.; Davies, S. N.; Geppetti, P.; Walker, J. M.; Di Marzo, V. An endogenous capsaicin-like substance with high potency at recombinant and native vanilloid VR1 receptors. *Proc. Natl. Acad. Sci. U.S.A.* **2002**, *99*, 8400−8405.
(11) Gaoni, Y.; Mechoulam, R. Isolation, Structure, and Partial Synthesis of an Active Constituent of Hashish. *J. Am. Chem. Soc.* **1964**, *86*, 1646−1647.
(12) Baker, D.; Pryce, G.; Giovannoni, G.; Thompson, A. J. The terapeutic potential of cannabis. *Lancet Neurol.* **2003**, *2*, 291−298.
(13) Bramblett, R. D.; Panu, A. M.; Ballesteros, J. A.; Reggio, P. H. Construction of a 3D model of the cannabinoid CB1 receptor: determination of helix ends and helix orientation. *Life Sci.* **1995**, *56*, 1971−1982.
(14) Song, Z. H.; Slowey, C. A.; Hurst, D. P.; Reggio, P. H. The difference between the CB(1) and CB(2) cannabinoid receptors at position 5.46 is crucial for the selectivity of WIN55212-2 for CB(2). *Mol. Pharmacol.* **1999**, *56*, 834−840.
(15) Schertler, G. F.; Villa, C.; Henderson, R. Projection structure of rhodopsin. *Nature* **1993**, *362*, 770−772.
(16) Baldwin, J. M. The probable arrangement of the helices in G protein-coupled receptors. *EMBO J.* **1993**, *12*, 1693−1703.
(17) McAllister, S. D.; Tao, Q.; Barnett-Norris, J.; Buehner, K.; Hurst, D. P.; Guarnieri, F.; Reggio, P. H.; Nowell Harmon, K. W.; Cabral, G. A.; Abood, M. E. A critical role for a tyrosine residue in the cannabinoid receptors for ligand recognition. *Biochem. Pharmacol.* **2002**, *63*, 2121−2136.
(18) Mahmoudian, M. The cannabinoid receptor: computer-aided molecular modeling and docking of ligand. *J. Mol. Graph. Model.* **1997**, *15*, 149−153, 179.
(19) Zhang, D.; Weinstein, H. Polarity conserved positions in transmembrane domains of G-protein coupled receptors and bacteriorhodopsin. *FEBS Lett.* **1994**, *337*, 207−212.
(20) Palczewski, K.; Kumasaka, T.; Hori, T.; Behnke, C. A.; Motoshima, H.; Fox, B. A.; Le Trong, I.; Teller, D. C.; Okada, T.; Stenkamp, R. E.; Yamamoto, M.; Miyano, M. Crystal structure of rhodopsin: A G protein-coupled receptor. *Science* **2000**, *289*, 739−745.
(21) Ballesteros, J.; Palczewski, K. G protein-coupled receptor drug discovery: implications from the crystal structure of rhodopsin. *Curr. Opin. Drug Discovery Dev.* **2001**, *4*, 561−574.
(22) Ballesteros, J. A.; Shi, L.; Javitch, J. A. Structural mimicry in G protein-coupled receptors: implications of the high-resolution structure of rhodopsin for structure−function analysis of rhodopsin-like receptors. *Mol. Pharmacol.* **2001**, *60*, 1−19.
(23) Bissantz, C.; Bernard, P.; Hibert, M.; Rognan, D. Protein-based virtual screening of chemical databases. II. Are homology models of G-Protein Coupled Receptors suitable targets? *Proteins* **2003**, *50*, 5−25.
(24) Barnett-Norris, J.; Hurst, D. P.; Lynch, D. L.; Guarnieri, F.; Makriyannis, A.; Reggio, P. H. Conformational memories and the endocannabinoid binding site at the cannabinoid CB1 receptor. *J. Med. Chem.* **2002**, *45*, 3649−3659.
(25) Shim, J. Y.; Welsh, W. J.; Howlett, A. C. Homology model of the CB1 cannabinoid receptor: Sites critical for nonclassical cannabinoid agonist interaction. *Biopolymers* **2003**, *71*, 169−189.
(26) Baldwin, J. M.; Schertler, G. F.; Unger, V. M. An alpha-carbon template for the transmembrane helices in the rhodopsin family of G-protein-coupled receptors. *J. Mol. Biol.* **1997**, *272*, 144−164.
(27) Mirzadegan, T.; Benko, G.; Filipek, S.; Palczewski, K. Sequence analyses of G-protein-coupled receptors: similarities to rhodopsin. *Biochemistry* **2003**, *42*, 2759−2767.
(28) Gouldson, P.; Calandra, B.; Legoux, P.; Kerneis, A.; Rinaldi-Carmona, M.; Barth, F.; Le Fur, G.; Ferrara, P.; Shire, D. Mutational analysis and molecular modelling of the antagonist SR 144528 binding site on the human cannabinoid CB(2) receptor. *Eur. J. Pharmacol.* **2000**, *401*, 17−25.
(29) Shire, D.; Calandra, B.; Bouaboula, M.; Barth, F.; Rinaldi-Carmona, M.; Casellas, P.; Ferrara, P. Cannabinoid receptor interactions with the antagonists SR 141716A and SR 144528. *Life Sci.* **1999**, *65*, 627−635.
(30) Shire, D.; Calandra, B.; Delpech, M.; Dumont, X.; Kaghad, M.; Le Fur, G.; Caput, D.; Ferrara, P. Structural features of the central cannabinoid CB1 receptor involved in the binding of the specific CB1 antagonist SR 141716A. *J. Biol. Chem.* **1996**, *271*, 6941−6946.
(31) Kleywegt, G. J.; Jones, T. A. Phi/Psi-chology: Ramachandran revisited. *Structure* **1996**, *4*, 1395−1400.
(32) Reggio, P. H. Pharmacophores for ligand recognition and activation/inactivation of the cannabinoid receptors. *Curr. Pharm. Des.* **2003**, *9*, 1607−1633.
(33) Jensen, A. D.; Guarnieri, F.; Rasmussen, S. G. F.; Asmar, F.; Ballesteros, J. A.; Gether, U. Agonist-induced conformational changes at the cytoplasmic side of transmembrane segment 6 in the beta(2) adrenergic receptor mapped by site-selective fluorescent labeling. *J. Biol. Chem.* **2001**, *276*, 9279−9290.
(34) Barnett-Norris, J.; Hurst, D. P.; Buehner, K.; Ballesteros, J. A.; Guarnieri, F.; Reggio, P. H. Agonist alkyl tail interaction with cannabinoid CB1 receptor V6.43/I6.46 groove induces a helix 6 active conformation. *Int. J. Quantum Chem.* **2002**, *88*, 76−86.

(35) Singh, R.; Hurst, D. P.; Barnett-Norris, J.; Lynch, D. L.; Reggio, P. H.; Guarnieri, F. Activation of the cannabinoid CB1 receptor may involve a W6.48/F3.36 rotamer toggle switch. *J. Pept. Res.* **2002**, *60*, 357−370.
(36) Song, Z. H.; Bonner, T. I. A lysine residue of the cannabinoid receptor is critical for receptor recognition by several agonists but not WIN55212-2. *Mol. Pharmacol.* **1996**, *49*, 891−896.
(37) McAllister, S. D.; Hurst, D.; Buehner, K.; Norris, J. B.; Reggio, P. H.; Abood, M. E. Aromatic residues in helixes 3-5-6 of CB1 provide specific interaction sites for WIN55,212-2 and SR141716A. *2002 Symposium on the Cannabinoids*; International Cannabinoid Research Society, Burlington, VT, 2002; p 76.
(38) McAllister, S. D.; Rizvi, G.; Anavi-Goffer, S.; Hurst, D. P.; Barnett-Norris, J.; Lynch, D. L.; Reggio, P. H.; Abood, M. E. An aromatic microdomain at the cannabinoid CB(1) receptor constitutes an agonist/inverse agonist binding region. *J. Med. Chem.* **2003**, *46*, 5139−5152.
(39) Huffman, J. W.; Yu, S.; Showalter, V.; Abood, M. E.; Wiley: J. L.; Compton, D. R.; Martin, B. R.; Bramblett, R. D.; Reggio, P. H. Synthesis and pharmacology of a very potent cannabinoid lacking a phenolic hydroxyl with high affinity for the CB2 receptor. *J. Med. Chem.* **1996**, *39*, 3875−3877.
(40) Hart, R.; Hurst, D. P.; Reggio, P. The CB1 TMH 2-3 region forms the binding site for (+)-7-OH-CBD-DMH. *2003 Symposium on the Cannabinoids*; International Cannabinoid Research Society, Burlington, VT, 2003; p 76.
(41) Huffman, J. W.; Mabon, R.; Wu, M. J.; Lu, J.; Hart, R.; Hurst, D. P.; Reggio, P. H.; Wiley, J. L.; Martin, B. R. 3-Indolyl-1-naphthylmethanes: new cannabimimetic indoles provide evidence for aromatic stacking interactions with the CB(1) cannabinoid receptor. *Bioorg. Med. Chem.* **2003**, *11*, 539−549.
(42) Shim, J. Y.; Howlett, A. Prediction of the CB1 cannabinoid receptor region critical for the binding of aminoalkylindole (AAI) WIN55212-2. *2003 Symposium on the Cannabinoids*; International Cannabinoid Research Society, Burlington, VT, 2003; p 9.
(43) Chin, C. N.; Lucas-Lenard, J.; Abadji, V.; Kendall, D. A. Ligand binding and modulation of cyclic AMP levels depend on the chemical nature of residue 192 of the human cannabinoid receptor 1. *J. Neurochem.* **1998**, *70*, 366−373.
(44) MacLennan, S. J.; Reynen, P. H.; Kwan, J.; Bonhaus, D. W. Evidence for inverse agonism of SR141716A at human recombinant cannabinoid CB1 and CB2 receptors. *Br. J. Pharmacol.* **1998**, *124*, 619−622.
(45) Shim, J. Y.; Welsh, W. J.; Cartier, E.; Edwards, J. L.; Howlett, A. C. Molecular interaction of the antagonist N-(piperidin-1-yl)-5-(4-chlorophenyl)-1-(2,4-dichlorophenyl)-4-methyl-1H-pyrazole-3-carboxamide with the CB1 cannabinoid receptor. *J. Med. Chem.* **2002**, *45*, 1447−1459.
(46) Hurst, D. P.; Lynch, D. L.; Barnett-Norris, J.; Hyatt, S. M.; Seltzman, H. H.; Zhong, M.; Song, Z. H.; Nie, J.; Lewis, D.; Reggio, P. H. N-(piperidin-1-yl)-5-(4-chlorophenyl)-1-(2,4-dichlorophenyl)-4-methyl-1H-pyrazole-3-carboxamide (SR141716A) interaction with LYS 3.28(192) is crucial for its inverse agonism at the cannabinoid CB1 receptor. *Mol. Pharmacol.* **2002**, *62*, 1274−1287.
(47) Bairoch, A.; Apweiler, R. The SWISS-PROT protein sequence database and its supplement TrEMBL in 2000. *Nucleic Acids Res.* **2000**, *28*, 45−48.
(48) Berman, H. M.; Battistuz, T.; Bhat, T. N.; Bluhm, W. F.; Bourne, P. E.; Burkhardt, K.; Feng, Z.; Gilliland, G. L.; Iype, L.; Jain, S.; Fagan, P.; Marvin, J.; Padilla, D.; Ravichandran, V.; Schneider, B.; Thanki, N.; Weissig, H.; Westbrook, J. D.; Zardecki, C. The Protein Data Bank. *Acta Crystallogr. D Biol. Crystallogr.* **2002**, *58*, 899−907.
(49) Thompson, J. D.; Higgins, D. G.; Gibson, T. J. CLUSTAL W: improving the sensitivity of progressive multiple sequence alignment through sequence weighting, position-specific gap penalties and weight matrix choice. *Nucleic Acids Res.* **1994**, *22*, 4673−4680.
(50) CLUSTAL W (version 1.82): http://www.ebi.ac.uk/clustalw/ (default settings: matrix, Blosum series; gap opening penalty, 10; gap extension penalty, 0.05).
(51) *Sybyl v. 6.9*; Tripos Associates, Inc.: St. Louis, MO.
(52) *InsightII v. 2000*; Accelrys, Inc.: San Diego, CA.
(53) Weiner, S. J.; Kollman, P. A.; Case, D. A.; Singh, U. C.; Ghio, C.; Alagona, G.; Profeta, S.; Weiner, J. P. A new force field for molecular mechanical simulation of nucleic acids and proteins. *J. Am. Chem. Soc.* **1984**, *106*, 765−784.
(54) Weiner, S. J.; Kollman, P. A.; Nguyen, D. T.; Case, D. A. An all atom force field for simulations of proteins and nucleic acids. *J. Comput. Chem.* **1986**, *7*, 230−252.
(55) Besler, B. H.; Merz, K. M.; Kollman, P. A. Atomic charges derived from semiempirical methods. *J. Comput. Chem.* **1990**, *11*, 431−439.
(56) *GROMACS, v. 3.1.4*; Department of Biophysical Chemistry, University of Groningen, Nijenborgh 4, 9747 AG Groningen, The Netherlands (http://www.gromacs.org/).
(57) Lindahl, E.; Hess, B.; van der Spoel, D. GROMACS 3.0: A package for molecular simulation and trajectory analysis. *J. Mol. Mod.* **2001**, *7*, 306−317.
(58) *GOLD v. 2.0*; Cambridge Crystallographic Data Centre: Cambridge, U.K.
(59) CScore: http://www.tripos.com/sciTech/inSilicoDisc/virtualScreening/cscore.html#references.
(60) Laskowski, R. A.; MacArthur, M. W.; Moss, D. S.; Thornton, J. M. PROCHECK: a program to check the stereochemical quality of protein structures. *J. Appl. Crystallogr.* **1993**, *26*, 283−291.
(61) Ballesteros, J. A.; Weinstein, H. W. Integrated methods for the construction of three-dimensional models and computational probing of structure−function relations in G-protein coupled receptors. In *Methods in Neuroscience*; Sealfon, S. C., Ed.; Academic Press: San Diego, 1995; pp 366−428.
(62) Teller, D. C.; Okada, T.; Behnke, C. A.; Palczewski, K.; Stenkamp, R. E. Advances in determination of a high-resolution three-dimensional structure of rhodopsin, a model of G-protein-coupled receptors (GPCRs). *Biochemistry* **2001**, *40*, 7761−7772.
(63) Altschul, S. F.; Madden, T. L.; Schaffer, A. A.; Zhang, J.; Zhang, Z.; Miller, W.; Lipman, D. J. Gapped BLAST and PSI-BLAST: a new generation of protein database search programs. *Nucleic Acids Res.* **1997**, *25*, 3389−3402.
(64) PSI-BLAST: http://www.ncbi.nlm.nih.gov/BLAST/ (default settings; matrix, Blosum62).
(65) SWISS-PROT: CB1R_HUMAN (P21554), CB1R_RAT (P20272), CB1R_FELCA (O02777), CB1R_POEGU (P56971), CB1R_TARGR (Q9PUI7), CB1A_FUGRU (Q98894), CB1B_FUGRU (Q98895), CB2R_RAT (Q9QZN9), CB2R_MOUSE (P47936), CB2R_HUMAN (P34972), HH1R_BOVIN (P30546), EDG1_RAT (P48303), MC5R_RAT (P35345), OPSD_BOVIN (P02699).
(66) Essman, U.; Perela, L.; Berkowitz, M. L.; Darden, T.; Lee, H.; Pedersen, L. G. A smooth particle mesh Ewald method. *J. Chem. Phys.* **1995**, *103*, 8577−8592.
(67) Berendsen, H. J. C.; Postma, J. P. M.; DiNola, A.; Haak, J. R. Molecular dynamics with coupling to an external bath. *J. Chem. Phys.* **1984**, *81*, 3684−3690.
(68) Jorgensen, W. L.; Chandrasekhar, J.; Madura, J. D.; Impey, R. W.; Klein, M. L. Comparison of simple potential functions for simulating liquid water. *J. Chem. Phys.* **1983**, *79*, 926−935.
(69) Jorgensen, W. L.; Maxwell, D. S.; Tirado-Rives, J. Development and testing of the OPLS all-atom force field on conformational energetics and properties of organic liquids. *J. Am. Chem. Soc.* **1996**, *118*, 11225−11236.
(70) Kony, D.; Damm, W.; Stoll, S.; Van Gunsteren, W. F. An improved OPLS-AA force field for carbohydrates. *J. Comput. Chem.* **2002**, *23*, 1416−1429.
(71) van Gunsteren, W. F.; Berendsen, H. J. C. *Gromos-87 manual*; Biomos BV Nijenborgh 4, 9747 AG Groningen, The Netherlands, 1987.
(72) *Visual Data*; Visipoint Oy, Kuopio, Finland (http://www.visipoint.fi).
(73) Kohonen, T. *Self-Organizing Maps*, 2nd ed.; Springer-Verlag: Berlin, 1997.
(74) McDonald, I. K.; Thornton, J. M. Satisfying hydrogen bonding potential in proteins. *J. Mol. Biol.* **1994**, *238*, 777−793.
(75) Burley, S. K.; Petsko, G. A. Aromatic−aromatic interaction: a mechanism of protein structure stabilization. *Science* **1985**, *229*, 23−28.
(76) Hunter, C. A.; Singh, J.; Thornton, J. M. Pi−pi interactions: the geometry and energetics of phenylalanine-phenylalanine interactions in proteins. *J. Mol. Biol.* **1991**, *218*, 837−846.
(77) Connolly, M. L. Solvent-accessible surfaces of proteins and nucleic acids. *Science* **1983**, *221*, 709−713.

JM031052C